British Journal of Pharmacology

British Journal of Pharmacology (2016) **173** 1095–1109 1095

RESEARCH PAPER

Fenofibrate inhibits atrial metabolic remodelling in atrial fibrillation through PPAR-α/sirtuin 1/PGC-1α pathway

Correspondence Wei-min Li or Yue Li, Department of Cardiology, the First Affiliated Hospital of Harbin Medical University, Youzheng Street 23#, Nangang District, Harbin 150001, Heilongjiang Province, China. E-mail: liweimin_2009@163.com or ly99ly@vip.163.com

Received 30 July 2015; **Revised** 9 January 2016; **Accepted** 13 January 2016; **accepted Article Published Online**
18 February 2016

Guang-zhong Liu[1], Ting-ting Hou[1], Yue Yuan[1], Peng-zhou Hang[2], Jing-jing Zhao[1], Li Sun[1], Guan-qi Zhao[1], Jing Zhao[3], Jing-mei Dong[1], Xiao-bing Wang[1], Hang Shi[1], Yong-wu Liu[4], Jing-hua Zhou[5], Zeng-xiang Dong[3], Yang Liu[1], Cheng-chuang Zhan[1], Yue Li[1,3] and Wei-min Li[1,3]

[1]Department of Cardiology, The First Affiliated Hospital of Harbin Medical University, Harbin, Heilongjiang Province, China, [2]Institute of Clinical Pharmacology, The Second Affiliated Hospital of Harbin Medical University, Harbin, Heilongjiang Province, China, [3]Key Laboratory of Cardiac Diseases and Heart, Failure of Harbin Medical University, Harbin, Heilongjiang Province, China, [4]Centre for Drug Safety Evaluation, Heilongjiang University of Chinese Medicine, Harbin, Heilongjiang Province, China, and [5]Department of Morphology, Heilongjiang University of Chinese Medicine, Harbin, Heilongjiang Province, China

BACKGROUND AND PURPOSE

Atrial metabolic remodelling is critical for the process of atrial fibrillation (AF). The PPAR-α/sirtuin 1 /PPAR co-activator α (PGC-1α) pathway plays an important role in maintaining energy metabolism. However, the effect of the PPAR-α agonist fenofibrate on AF is unclear. Therefore, the aim of this study was to determine the effect of fenofibrate on atrial metabolic remodelling in AF and explore its possible mechanisms of action.

EXPERIMENTAL APPROACH

The expression of metabolic proteins was examined in the left atria of AF patients. Thirty-two rabbits were divided into sham, AF (pacing with 600 beats·min^{-1} for 1 week), fenofibrate treated (pretreated with fenofibrate before pacing) and fenofibrate alone treated (for 2 weeks) groups. HL-1 cells were subjected to rapid pacing in the presence or absence of fenofibrate, the PPAR-α antagonist GW6471 or sirtuin 1-specific inhibitor EX527. Metabolic factors, circulating biochemical metabolites, atrial electrophysiology, adenine nucleotide levels and accumulation of glycogen and lipid droplets were assessed.

KEY RESULTS

The PPAR-α/sirtuin 1/PGC-1α pathway was significantly inhibited in AF patients and in the rabbit/HL-1 cell models, resulting in a reduction of key downstream metabolic factors; this effect was significantly restored by fenofibrate. Fenofibrate prevented the alterations in circulating biochemical metabolites, reduced the level of adenine nucleotides and accumulation of glycogen and lipid droplets, reversed the shortened atrial effective refractory period and increased risk of AF.

CONCLUSION AND IMPLICATIONS

Fenofibrate inhibited atrial metabolic remodelling in AF by regulating the PPAR-α/sirtuin 1/PGC-1α pathway. The present study may provide a novel therapeutic strategy for AF.

Abbreviations

AcAc, acetoacetate; AERP, atrial effective refractory period; AF, atrial fibrillation; BOH, β-hydroxybutyrate; FFA, free fatty acid; GLUT4, glucose transporter 4; GS1, glycogen synthase1; H-FABP, heart fatty acid binding protein; MCAD, medium-chain acyl-CoA dehydrogenase; mCPT-1, mitochondrial carnitine palmitoyltransferase1; PDH, pyruvate dehydrogenase; PDK4, pyruvate dehydrogenase kinase 4; PGC-1α, PPAR co-activator 1α; p-GS1, phosphorylated-GS1; TKB, total ketone body

DOI:10.1111/bph.13438

Tables of Links

TARGETS	
Nuclear hormone receptors[a]	**Enzymes**[b]
PPAR-α	AMPK
Other protein targets	CaMKII
H-FABP	PDK4
Transporters[c]	Sirtuin 1
GLUT4	

LIGANDS	
Acetoacetate (AcAc)	ATP
Adenine	EX527 (selisistat)
ADP	Fenofibrate
AMP	GW6471

These Tables list key protein targets and ligands in this article which are hyperlinked to corresponding entries in http://www.guidetopharmacology.org, the common portal for data from the IUPHAR/BPS Guide to PHARMACOLOGY (Pawson *et al.*, 2014) and are permanently archived in the Concise Guide to PHARMACOLOGY 2015/16 ([a,b,c]Alexander *et al.*, 2015a,b,c).

Introduction

Atrial fibrillation (AF) is the most common sustained arrhythmia in clinical practice and may eventually cause heart failure and stroke. The initiation and progression of AF result from atrial remodelling, including electrical, structural and contractile remodelling, which has been shown to contribute continuously to the self-perpetuating nature of AF ('AF begets AF') (Casaclang-Verzosa *et al.*, 2008; Heijman *et al.*, 2014). Both experimental and clinical studies have suggested that disturbances in atrial energy metabolism are involved in the pathogenesis of AF (Ausma *et al.*, 2000; Mihm *et al.*, 2001). Recently, studies reported that metabolism-related proteins and key enzymes in energy metabolism were deregulated and transcripts involved in several glycolytic enzymes were up-regulated in human persistent AF (Barth *et al.*, 2005; Mayr *et al.*, 2008; Tu *et al.*, 2014). Moreover, the impairment of energy production or consumption was found during AF (Tsuboi *et al.*, 2001; Cha *et al.*, 2003; Seppet *et al.*, 2005). AMP-activated protein kinase (AMPK) is regarded as a sensor of metabolic stress. AMPK is activated to protect the atria against profibrillatory effects and compensate for the metabolic dysfunction in experimental AF (Harada *et al.*, 2015). However, AF induces the up-regulation of Ca^{2+}/calmodulin-dependent protein kinase II (CaMKII) and AMPK, resulting in lipid and glycogen accumulation (Lenski *et al.*, 2015). The understanding of the precise mechanism underlying the impact of cardiac metabolic remodelling on AF persistence remains limited.

Sirt1 (a homologue of yeast sir2 and NAD+ -dependent class-III histone/protein deacetylase, which is a shuttling protein between the nucleus and cytoplasm) is a key molecule in metabolic regulation (Guarente, 2006). Phospho-Sirtuin 1 (p-sirt1 activating form) is essential for its own enzyme activity and nuclear translocation, which is considered to be its primary protective role (Tanno *et al.*, 2007; Sasaki *et al.*, 2008; Tanno *et al.*, 2010). Importantly, sirtuin 1 plays a pivotal role in maintaining metabolic homoeostasis by up-regulating fatty acid oxidation genes, such as mitochondrial carnitine palmitoyltransferase1 (mCPT-1) and medium-chain acyl-CoA dehydrogenase (MCAD), and suppressing sterol regulatory element-binding protein-1 (SREBP-1) (Lagouge *et al.*, 2006). Furthermore, it is widely accepted that sirtuin 1 regulates PGC-1α activity, which is involved in the regulation of mitochondrial biogenesis and energy metabolism (Chang and Guarente, 2014).

The PPAR-α agonist fenofibrate is widely used for dyslipidaemia in the clinic. PPAR-α activation has been suggested to prevent the reduction in fatty acid metabolism genes and reverse cardiac dysfunction (Liang *et al.*, 2003; Lam *et al.*, 2015). Fenofibrate can reduce lipotoxicity in the pathological heart and kidney (Asai *et al.*, 2006; Hong *et al.*, 2014). Both PPAR-α and sirtuin 1 have emerged as interesting targets because they are positively involved in the regulation of fatty acid and glucose metabolism (Madrazo and Kelly, 2008; Chang and Guarente, 2014). PPAR-α and sirtuin 1 are regulated by fenofibrate (Wang *et al.*, 2015). However, the effects of fenofibrate on the atrial metabolic disturbance associated with AF are not completely understood. Therefore, our study was designed to investigate whether fenofibrate prevented atrial metabolic remodelling in AF through the PPAR-α/sirtuin 1/PGC-1α pathway.

Methods

Group sizes

To evaluate the effects of fenofibrate pretreatment before right atrial rapid-pacing stimulation, the rabbits were randomly divided into four groups: (1) sham operated group (sham group, n = 8) with sutured electrodes and no pacing; (2) pacing group (AF group, n = 8) with an AF model induced by rapid right atrial pacing for 1 week at 600 beats·min^{-1}; (3) fenofibrate treatment group (AF + FB group, n = 8) with fenofibrate-administered p.o. (Fournier, Daix, France) at a dose of 125 mg·kg^{-1}·day^{-1} for 14 days (Hennuyer *et al.*, 1999; Zhao *et al.*, 2014) and pacing the right atria for 1 week beginning on the eighth day; and (4) fenofibrate alone group (n = 8) with sutured electrodes and no pacing and only p.o. administration of fenofibrate (125 mg·kg^{-1}·day^{-1}) for 14 days.

Randomization

We used the random number table to perform the randomization. First, all rabbits were weighed and placed in order by wt

from light to heavy in the range 2.5–3.0 kg. Then, we chose a number from the random number table randomly and numbered that to the lightest rabbit. In total, four groups were needed; therefore, we divided the number by four. If this number was divided exactly by four, the rabbit would be put into the first group; if not, but with remainder 1, the rabbit would be allocated into the second group, and similarly, to the third and forth groups. After the lightest rabbit was grouped, the number on the right of the previous one in the random number table was given to the second rabbit, and the same methods were used to group this rabbit until all the rabbits had been allocated to a group.

Blinding
All the data were collected and analysed by two observers who were blinded to the group assignment of animals.

Normalization
The following data were normalized: biochemical measurements, atrial electrophysiology, quantitative analysis of Western blotting and the expression of genes. Moreover, for data sets of Western blotting and RT-PCR, all the data were adjusted to the values of the internal standard (such as GAPDH or β-actin). First, we calculated the control mean, and then all values in all groups respectively to the mean value of the experimental control group in order to set the Y-axis so the control group value is 1 or 100%, and all the individual test values as fold of control mean, and statistically analysis of these normalized values was conducted as appropriate (Curtis *et al.*, 2015). The Y-axis was labelled as fold of control mean. No data were used for transformation in our experiments.

Validity of animal species or model selection
In the present study, the AF model was established according to our previous studies (Li *et al.*, 2007; Liu *et al.*, 2013). Rabbits were chosen as a species to use in this study, because of their sensitivity to rapid-pacing-induced AF.

Animal studies
Animal studies are reported in compliance with the ARRIVE guidelines (Kilkenny *et al.*, 2010; McGrath and Lilley, 2015). The use of animals and all procedures were in agreement with the Guide for the Care and Use of Laboratory Animals (NIH Publication 2011, eighth edition) and were approved by the Animal Care and Use Committee of the Harbin Medical University (Harbin, China). All rabbits were raised in the SPF (specific pathogen free) animal centre of the First Affiliated Hospital of Harbin Medical University. All animals received a standard laboratory diet and filtered water *ad libitum*. They were housed in individual cages in a temperature-controlled room at 23°C under a 12 h light–dark cycle. Thirty-two New Zealand white rabbits (2.5–3.0 kg, male, Experimental Animal Centre of the First Affiliated Hospital of Harbin Medical University, Harbin, China) were used in this study.

Experimental procedures
The rabbits were anaesthetized with ketamine (30–35 mg·kg^{-1}) and xylazine (Sigma; 5 mg·kg^{-1} i.m.). All rabbit procedures were performed by sterile thoracotomy under mechanical ventilation. A bipolar electrode was attached to the right atrium and sutured. A pacemaker (AOO, Fudan University, Shanghai, China) was implanted in a s.c. pocket and connected with an electrode lead. The operations that could cause pain and distress were performed in another room without other animals present. All rabbits were allowed to recover for 1 week after the operation.

Interpretation
This study was carried out in complied with the replacement, refinement and reduction (the 3Rs).

Further methods

Patient selection
All patients recruited into the study provided informed consent for their samples to be used. The study complied with the principles that govern the use of human tissues outlined in the Declaration of Helsinki. Left atrial appendages were obtained as surgical specimens from patients undergoing cardiac surgery for mitral valve replacement following established procedures approved by the local Ethics Committee. Samples were collected from patients with sinus rhythm (SR, n = 6, without history of AF) and permanent AF (n = 6, documented arrhythmia for >6 months before surgery). Patients were excluded from the study if they had other cardiac diseases, such as severe congestive heart failure, or serious systemic diseases, such as thyroid disease, impaired glucose tolerance or diabetes mellitus. The specimens were immediately stored in liquid nitrogen and then fixed in 10% paraformaldehyde for 48 h at 4°C. The clinical subject characteristics were shown in Table 1.

Rabbit AF model
Thirty-two New Zealand white rabbits (2.5–3.0 kg, Experimental Animal Center of the First Affiliated Hospital of Harbin Medical University, Harbin, China) were randomly divided into four groups as stated above. The AF model was established according to our previous studies (Li *et al.*, 2007; Liu *et al.*, 2013). The rabbits were anaesthetized with ketamine (30–35 mg·kg^{-1}) and xylazine (Sigma; 5 mg·kg^{-1} i.m.). All rabbit procedures were performed by sterile thoracotomy under mechanical ventilation. A bipolar electrode was attached to the right atrium and sutured. A pacemaker (AOO, Fudan University, Shanghai, China) was implanted in a s.c. pocket and connected with an electrode lead. All rabbits were allowed to recover for 1 week after the operation. All blood samples were collected after an overnight fast, and serum was separated and stored at −80°C before analysis.

Cell culture
HL-1 cells were cultured in flasks in Claycomb medium (JRH Biosciences, Lenexa, KA, USA) supplemented with 10% foetal calf serum, 100 U·mL penicillin and 100 μL streptomycin (Gibco-BRL, Rockville, MD, USA). HL-1 cells (≥1 × 10^6 myocytes) were cultured in well plates and subjected to tachypacing by applying a YC-2 stimulator (Chengdu, China), as described in previous studies (Yang *et al.*, 2005; Brundel *et al.*, 2006). The cells

Table 1

Characteristics of the clinical subjects

	SR (n = 6)	PAF (n = 6)	P value
Age (years)	50.67 ± 3.55	58.17 ± 3.32	0.154
BW (kg)	72.33 ± 7.80	63.67 ± 5.71	0.391
BMI ($kg \cdot m^{-2}$)	24.83 ± 4.81	23.38 ± 4.35	0.596
Left atrial diameter (mm)	43.5 ± 1.95	54.33 ± 4.88	0.066
Right atrial diameter (up and down, mm)	49.33 ± 1.31	57.33 ± 3.47	0.0564
Right atrial diameter (left and right, mm)	36.83 ± 1.17	36.17 ± 3.89	0.87
EF (%)	61.00 ± 1.93	64.50 ± 3.45	0.397
Fasting blood glucose ($mmol \cdot L^{-1}$)	5.94 ± 0.69	5.68 ± 0.47	0.76
Total cholesterol ($mmol \cdot L^{-1}$)	4.66 ± 0.78	4.08 ± 0.29	0.418
Triglycerides ($mmol \cdot L^{-1}$)	1.19 ± 0.27	1.24 ± 0.77	0.886
Medication			
Spirolactone	6/6	6/6	
Furosemide	6/6	6/6	
Angiotensin II receptor blocker (ARB)	1/6	0/6	
NYHA class (II/III)	4/2	3/3	

[a]The data are expressed as mean ± SEM. SR, sinus rhythm.
[b]PAF, permanent atrial fibrillation; BW, body wt; BMI, body mass index; EF, ejection fraction; NYHA, New York Heart Association classification.

were stimulated at 10 Hz with square pulses of 5 ms duration and a pulse voltage set to 1.5 $V \cdot cm^{-1}$. The required capture efficiency was 90% of cells (microscopic examination of cell shortening) throughout the stimulation period.

Biochemical measurements

Blood samples were centrifuged at 3000–3500× g for 10–15 min. All procedures followed the manufacturer's instructions. Lactate, heart fatty acid binding protein (H-FABP) and free fatty acid (FFA) concentration measurement kits were obtained from Jiancheng Biological Technical Institute (China). Ketone body assay kits were provided by BioAssay Systems (EnzyChrom™, Hayward, CA, USA). The total ketone body (TKB) was calculated as acetoacetate (AcAc) + β-hydroxybutyrate (BOH) (Sharma *et al.*, 2011). Serum levels of total cholesterol (TC), triglycerides (TG), blood glucose, creatine kinase (CK) and creatine kinase isoenzyme-MB (CK-MB) were determined by the Roche Cobas c311 automatic biochemistry analyser (Tokyo, Japan).

Atrial electrophysiology

The atrial electrophysiology measurements were collected according to the method described in a previous study (Zhao *et al.*, 2010). Eight basic stimuli (S1) were followed by a premature extra stimulus (S2), and the S1S1 cycle had two basic cycle lengths (BCLs) (150 and 200 ms). The S1–S2 interval was increased by 5 ms and then decreased in 2 ms steps until S2 failed to capture the depolarization defined as the atrial Effective Refractory Period (AERP) value. The AERP value was measured three times at BCLs of 200 ms ($AERP_{200}$) and 150 ms ($AERP_{150}$) to obtain the mean value of the three AERPs. AF vulnerability was determined as the percentage of AF and the atrial arrhythmia recorded with an intracardiac electrode sustained for over 1 s induced by a train of 10 Hz, 2 ms stimuli to the right atrium at four times the threshold current.

Adenine nucleotide determination

The adenine acid concentrations in the atrial tissues were determined as previously described (Sellevold *et al.*, 1986). The atrial tissue block (50 mg) was homogenized and deproteinized in pre-cooled 0.4 M perchloric acid ($HClO_4$) to measure the ATP, ADP and AMP concentrations, which were expressed in $\mu mol \cdot g^{-1}$ wet wt ($\mu mol \cdot gwwt^{-1}$). A total of 300 μL of the supernatant was assessed by HPLC. Total adenine nucleotides (TAN) were calculated as ATP + ADP + AMP.

Immunohistochemical determination

Atria (including the appendage and free wall) tissue specimens were fixed in 10% formalin and processed for paraffin sections with a 3–5 μm thickness. First, the specimens were rehydrated in xylene and ethanol solutions. Then, the sections were incubated with an anti-sirtuin 1 (1:200; Cell Signaling Technology, Danvers, MA, USA), anti-glycogen synthase1 (GS1, 1:300; Biosynthesis Biotechnology, Beijing, China) anti-phosphoglycogen synthase1 (p-GS1, 1:300; Biosynthesis Biotechnology, Beijing, China), anti-PPAR-α (1:200), anti-PGC-1α (1:250 Abcam, Cambridge, MA, USA) anti-human p (ser^{47})-sirtuin 1 (1:200, Abcam, Cambridge, MA, USA), anti-rabbit p(ser^{47})-sirtuin 1(1:100, Biosynthesis-Biotechnology, Beijing, China), anti-glucose transporter 4 (GLUT4) (1:500; Abcam, Cambridge, MA, USA), anti-mCPT-1 (1:200; Abcam, Cambridge, MA, USA) or anti-MCAD (1:300; Abcam, Cambridge, MA, USA) antibody overnight at 4°C. The tissue sections were reacted with peroxidase-conjugated goat anti-rabbit IgG (1:1000, Abcam) or peroxidase-conjugated rabbit anti-goat IgG (1:1000, Zhongshan, Beijing, China) at 37°C for 10–20 min. Then, they

were visualized with a DAB-based colorimetric method (Li *et al.*, 2012). A Periodic acid Schiff (PAS) staining kit (BA-4044A, Baso, Baso Biotechnology, Zhuhai, China) was employed to evaluate the glycogen distribution in myocytes. The positive cell area density (defined as the positive cell area/total area of the field) was applied to determine the expression of the target proteins by the digital medical image analysis system (HPISA-1000, Olympus, Shinjuku, Japan). The accumulation of lipid droplets in cardiac myocytes was detected by the Oil Red O staining kit (BA4081, Baso, Biotechnology, Zhuhai, China). Briefly, 10 μm frozen sections were obtained from a Leica CM1850, Germany and dyed with the Oil red O reagent at room temperature for 5–10 min. Then, the sections were dyed with haematoxylin. The lipid droplets are shown in red and the nuclei in blue.

Real-time RT-PCR

Total RNA was extracted with TRIzol (CWbio. Co. Ltd, Beijing, China). The quantitative real-time reverse transcriptase-PCR (RT-PCR) was used to determine the gene expression of metabolic factors using previously described procedures (Seiler *et al.*, 2004; Liu *et al.*, 2013). The total RNAwas treated with RNase-free DNase I (CWbio. Co. Ltd, Beijing,China) for 30 min at 37°C, heated to 75°C for 5 min and then finally cooled to 4°C. The real-time PCR was performed on the 7500 Sequence Detection System (Applied Biosystems, Foster City, CA, USA).The primers of related genes used in the study are listed in Table 2.

Western blotting

Protein samples were separated by 8–12% SDS-PAGE. The Western blotting procedures were basically the same as those described in a previous study (Li *et al.*, 2012). The proteins were transferred to a PVDF membrane. Then, the membranes were incubated overnight at 4°C with primary antibodies against sirtuin 1 (1:300, Cell Signaling Technology), p-sirtuin 1 (1:1000), PPAR-α (1:300), PGC-1α (1:500), MCAD (1:1000), mCPT1 (1:1000), GLUT4 (1:1000), SREBP-1(1:100, Abcam) and GAPDH (1:1000, Zhongshan). The membranes were incubated with horseradish peroxidase-conjugated goat anti-rabbit or mouse anti-rabbit IgG (1:1000, Abcam). The Western blots were developed with the Super-Signal West Femto Chemiluminescent Substrate (Thermo Scientific, Waltham, MA, USA) and quantified by scanning densitometry (Chemi-DOC, Bio-Rad, Laboratories, Hercules, CA, USA).

Data and statistical analyses

All quantitative data are expressed as the mean ± SEM. Statistical significance between different groups was determined by an unpaired *t*-test for two groups or a one-way ANOVA with the Bonferroni's *post hoc* test to compare all pairs of columns for more than two groups. A value of $P < 0.05$ was considered statistically significant. The data and statistical analysis comply with the recommendations on experimental design and analysis in pharmacology (Curtis *et al.*, 2015).

Drugs

EX527 was obtained from Tocris Bioscience (Tocris Bioscience, Bristol, UK), fenofibrate and GW6471 were obtained from Sigma-Aldrich (St Louis, MO, USA).

Table 2

Primers for real-time PCR

Gene name	Primer sequences	Product size (bp)
Sirt1 forward primer	CTTGTGGAAGTAACAGTGATAGTGG	159
Sirt1 reverse primer	GACCTCCATCAGCCCCAAA	
PPAR-α forward primer	CTACGAGGCCTACCTGAAGAACTT	134
PPAR-α reverse primer	CGAGCGTCTTCTCAGCCATAC	
MCAD forward primer	CCTAAGGCTCCTGCCAGTAAA	178
MCAD reverse primer	AACCAGCTCCCTCACCAAGTAA	
SREBP-1 forward primer	AAACTGCCCATCCACCGACT	170
SREBP-1 reverse primer	TTCAGCTTTGCCTCAGTGCC	
PGC-1α forward primer	TGATGACAGCGAAGATGAAAGTG	133
PGC-1α reverse primer	TTTGGGTGGTGACACGGAAT	
mCPT-1 forward primer	CTTTGACCGACACCTGTTTGC	116
mCPT-1 reverse primer	TGGTGGACAGGATGTTGTGGTT	
GLUT4 forward primer	GGCTTTGTGGCGTTCTTTGA	132
GLUT4 reverse primer	GATGAAGTTGCACGTCCAGTTG	
PDK4 forward primer	CTTCAGTTACACATACTCCACCGC	86
PDK4 reverse primer	GTAACCCGTAACCGAAACCAG	
PDH forward primer	GCCAATCATAAAAGACGCTG	150
PDH reverse primer	ATGCCAAACATCCCCAAGT	
β-actin forward primer	AGATCGTGCGGGACATCAAG	182
β-actin reverse primer	CAGGAAGGAGGGCTGGAAGA	

Results

Alterations of key metabolic factors in AF patients

We examined the protein expression of key metabolic factors in left atrial appendages from SR and AF patients (Figure 1). The mCPT1, MCAD and GLUT4 protein levels were significantly down-regulated in the AF patients (Figure 1A–1E), whereas SREBP1 was significantly increased in the AF patients (Figure 1F). Collectively, these findings indicated that AF contributed to the reduction in fatty acid oxidation and the transportation of glucose. We also found that the levels of PPAR-α, p-sirtuin 1 and PGC-1α were significantly down-regulated in the AF patients compared with the SR patients. However, no significant difference in sirtuin 1 expression was found between the SR and AF groups (Figure 2A–2D).

Fenofibrate reversed the AF-induced alterations in circulating biochemical metabolites

As shown in Table 3, no significant difference was observed in the blood glucose, TG or TC between the sham and AF groups. In contrast, we found that the concentrations of serum AcAc and BOH were markedly increased in the AF rabbits compared with the sham rabbits at the baseline level. Fenofibrate attenuated the AF-induced elevation in the AcAc and BOH levels. Moreover, the TKB level was significantly increased in the AF group compared with the sham group, which were reversed by fenofibrate. The serum lactate level in the AF group was significantly higher compared with the sham group; however, the lactate level was markedly reduced in the fenofibrate treated group compared with the AF group, indicating that glycolysis was significantly increased during AF.

Additionally, the H-FABP and FFA levels were significantly increased in the AF group compared with the sham group. Fenofibrate application resulted in a reduction in H-FABP and FFA compared with the AF group (Table 3). Furthermore, rapid pacing significantly elevated the serum CK and CK-MB levels compared with the sham group. Fenofibrate prevented the rapid pacing-induced elevation in CK and CK-MB levels (Table 3).

Electrophysiological measurements

The tendency for a rabbit to show signs of AF was dramatically increased in the AF group compared with the sham rabbits at baseline. However, the incidences of AF were markedly decreased after fenofibrate treatment (Figure 3B). $AERP_{150}$ and $AERP_{200}$ were significantly reduced in the AF rabbits compared with the sham rabbits at baseline. Treatment with

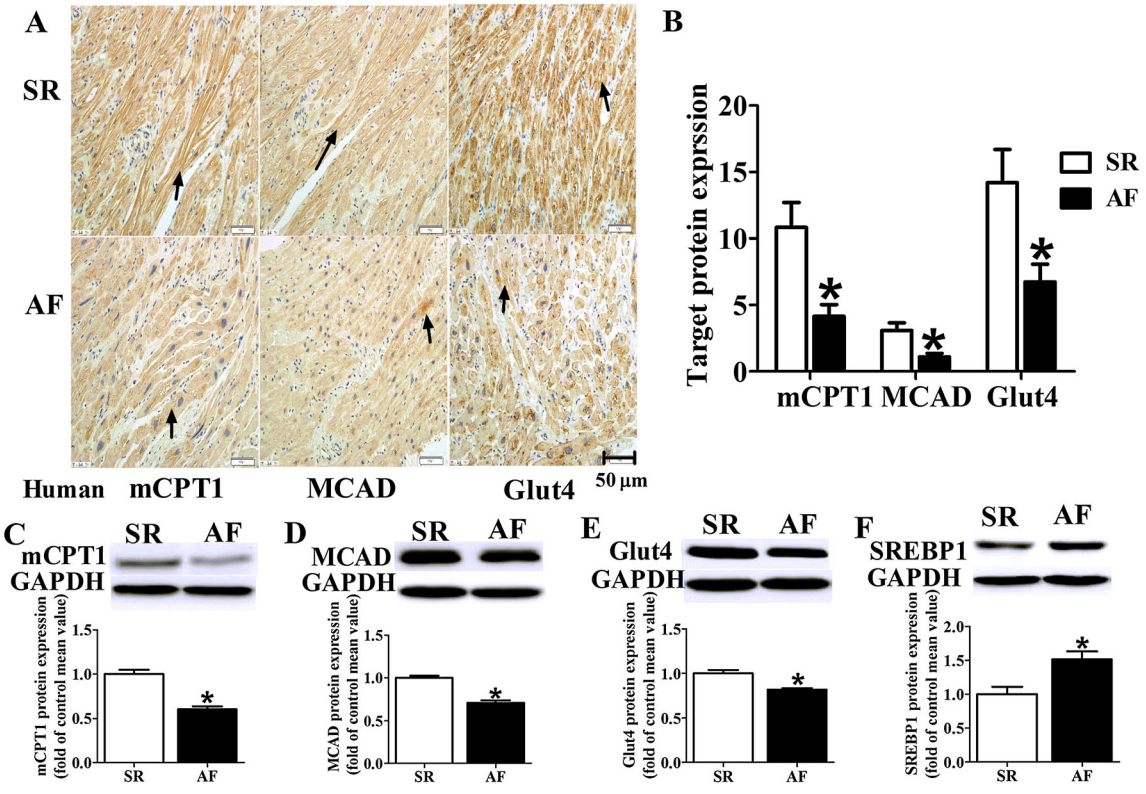

Figure 1

Alterations in the expression of key metabolic factors in the atria of patients with SR or AF. (A) Representative images of the protein expression of mitochondrial carnitine palmitoyltransferase1 (mCPT1), medium-chain acyl-CoA dehydrogenase (MCAD) and glucose transporter type 4 (GLUT4) in the atria of patients. (B) Quantitative analysis of the expression of mCPT1, MCAD and GLUT4 proteins in the atria. (C–F) Representative bands and quantitative analysis of mCPT1, MCAD, GLUT4 and sterol regulatory element binding protein1 (SREBP1) protein expression. The magnification is ×20. *$P < 0.05$ versus SR group, $n = 6$ per group.

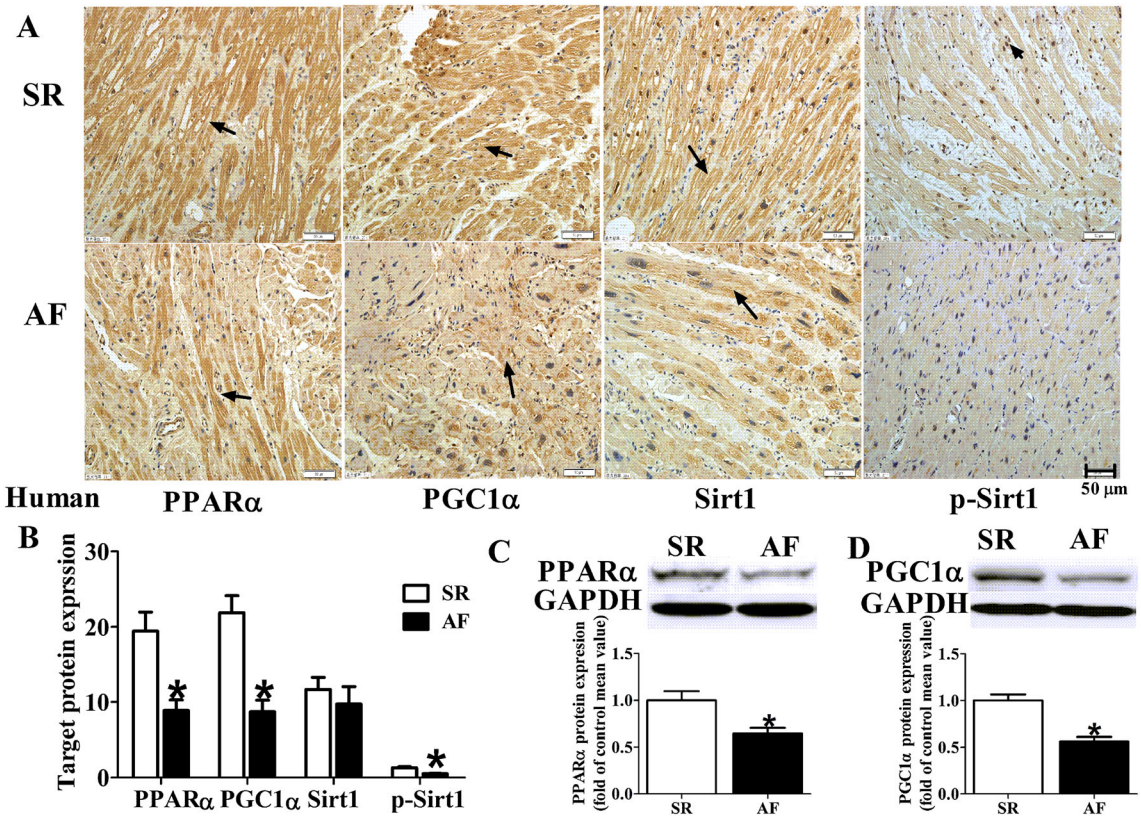

Figure 2

Down-regulation of PPAR-α, PGC-1α and phospho-sirtuin 1 expression in AF patients. (A, B) Representative images and quantitative analysis of PPAR-α, PGC-1α, sirtuin 1 and phospho-sirtuin 1 (p-Sirt1) expression in the atria of patients with SR or AF. (C, D) Representative band quantitative analysis of the expression of PPAR-α and PGC-1α in the atria of patients. The magnification is ×20. *$P < 0.05$ versus SR group, $n = 6$ per group.

Table 3

Changes in serum biochemical metabolites

Groups	sham	AF	AF + FB	FB
Blood glucose (mmol·L^{-1})	7.12 ± 0.50	8.05 ± 0.44	7.89 ± 0.49	7.03 ± 0.33
TG (mmol·L^{-1})	1.91 ± 0.12	1.66 ± 0.18	1.33 ± 0.19	1.18 ± 0.13
TC (mmol·L^{-1})	1.86 ± 0.14	1.61 ± 0.18	1.31 ± 0.19	1.71 ± 0.25
AcAc (mmol·L^{-1})	1.59 ± 0.19	3.59 ± 0.48*	2.50 ± 0.34	2.21 ± 0.52
BOH (mmol·L^{-1})	0.48 ± 0.04	1.38 ± 0.25*	0.81 ± 0.18$^{\#}$	0.64 ± 0.08
TKB (mmol·L^{-1})	2.07 ± 0.16	5.07 ± 0.31*	3.18 ± 0.39$^{\#}$	2.85 ± 0.48
Lactate (mmol·L^{-1})	2.89 ± 0.23	5.43 ± 0.33*	4.01 ± 0.35$^{\#}$	3.55 ± 0.19
H-FABP (ng·L^{-1})	57.34 ± 5.67	259.4 ± 32.11*	148.2 ± 17.87$^{\#}$	68.91 ± 7.15
FFA (μmol·L^{-1})	302.7 ± 44.93	1120 ± 108.5*	778.1 ± 79.73$^{\#}$	309.5 ± 40.28
CK (U·L^{-1})	467.8 ± 17.42	1345 ± 122.5*	1003 ± 104.1$^{\#}$	666.8 ± 105.0
CK-MB (U·L^{-1})	134.1 ± 9.83	293.9 ± 23.56*	224.3 ± 16.44$^{\#}$	163.3 ± 20.89

[a]The data were represented as mean ± SEM.
[b]TG, triglyceride; TC, total cholesterol; AcAc, acetoacetic acid; BOH, β-hydroxybutyrate; TKB, total ketone body = AcAc + BOH; H-FABP, heart-type fatty Acid binding protein; FFA, free fatty acid; CK, creatine kinase; CK-MB, creatinine kinase isoenzyme MB.
$^{*}P < 0.05$ versus sham group,
$^{\#}P < 0.05$ versus AF group, $n = 7$ per group.

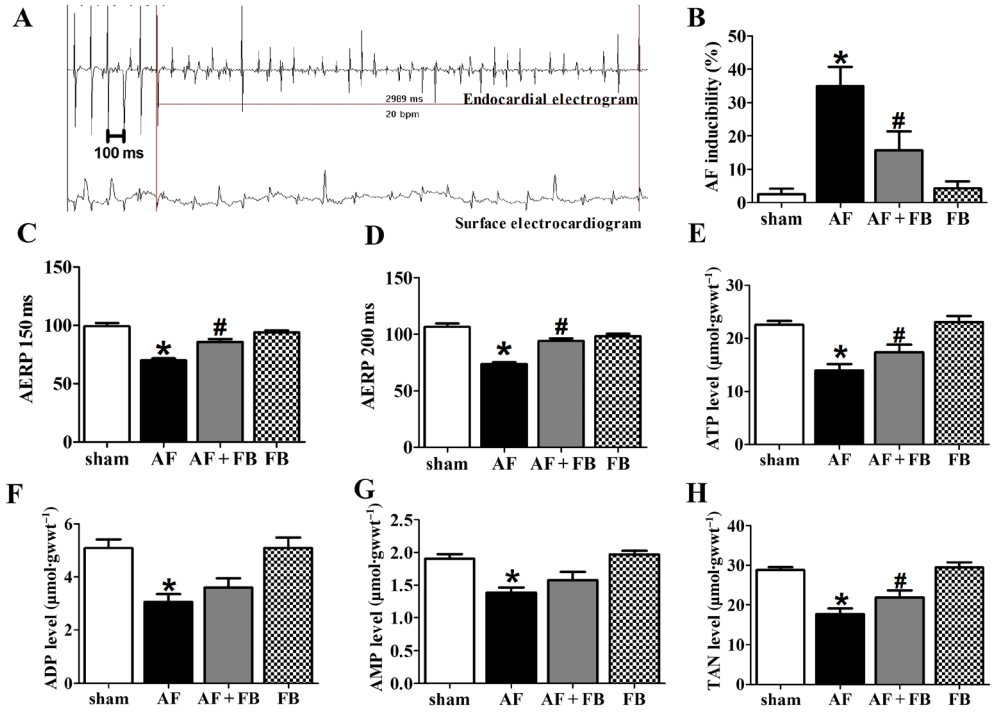

Figure 3

Fenofibrate (FB) reversed the AF-induced AERP and adenine nucleotide reduction. (A) AF was induced after rapid-pacing. (B) AF inducibility. (C, D) $AERP_{150\ ms}$ and $AERP_{200\ ms}$, $n = 8$ per group. (E–H) Quantitative analysis of the ATP, ADP, AMP and TAN levels in the atria of rabbits. *$P < 0.05$ versus sham group, #$P < 0.05$ versus AF group, $n = 6$ per group.

fenofibrate reversed the rapid pacing-induced $AERP_{150}$ and $AERP_{200}$ shortening in the AF + fenofibrate group compared with the AF group (Figure 3C,D).

Adenine nucleotide concentrations

The ATP, ADP and AMP concentrations were markedly decreased in the AF group compared with the sham group (Figure 3E–3G). The ATP, ADP and AMP levels in the AF + FB group were higher than the levels in the AF group (Figure 3E–3G). Moreover, the total adenine nucleotide (TAN) pool level was significantly reduced in the AF group of rabbits compared with the sham group of rabbits (Figure 3H). Significant differences in TAN were found between the AF and AF + FB groups (Figure 3H).

The effect of fenofibrate on the accumulation of glycogen and lipid droplets

Abnormal glycogen accumulation is an important indicator of AF metabolic remodeling. PAS staining showed that AF induced an increase in glycogen accumulation in the atria, as shown in Figure 4A. A large number of red granules were observed in the cardiac tissue; this accumulation was partially attenuated by fenofibrate. Similarly, Oil red O staining detected lipid droplets in the atria among the groups (Figure 4D). The rapid atrial pacing resulted in a notable accumulation of lipid droplets (indicated with black arrows in Figure 4D). However, fenofibrate significantly reduced this accumulation of lipid droplets. Immunohistochemical staining showed that GS1 was significantly increased in the AF group compared with the sham group (Figure 4B), whereas p-GS1 was markedly reduced (Figure 4C); this effect was reversed by fenofibrate. These findings indicate that AF induced GS1 expression and inhibited the up-regulation of p-GS1. Thus, fenofibrate could improve the imbalance in GS1/p-GS1 expression and reduce the accumulation of glycogen.

Fenofibrate inhibited the AF-induced remodelling of key metabolic factors

Exposure of the atria in rabbits to rapid pacing obviously decreased the protein and gene expression levels of mCPT-1 and MCAD and increased SREBP1 expression; these effects were attenuated by fenofibrate (Figure 5A–5C). Next, we detected the mRNA and protein levels of crucial regulators of glucose metabolism, including GLUT4, pyruvate dehydrogenase (PDH) and pyruvate dehydrogenase kinase 4 (PDK4). AF significantly inhibited the expression of GLUT4 and PDH and enhanced PDK4 mRNA expression; these changes in expression were restored by fenofibrate (Figure 5B,5D).

Fenofibrate attenuated the down-regulation of the PPAR-α/sirtuin 1/PGC-1α proteins during AF

Figure 6 shows that the mRNA and protein expression levels of PPAR-α, PGC-1α and p-sirtuin 1 were significantly reduced in the AF rabbits, although the alterations in sirtuin 1 mRNA and protein expression levels were not significant compared with the sham group. Fenofibrate reversed the down-regulation of these key metabolic regulators (Figure 6A–6F). Similarly, HL-1 cells were pretreated with fenofibrate

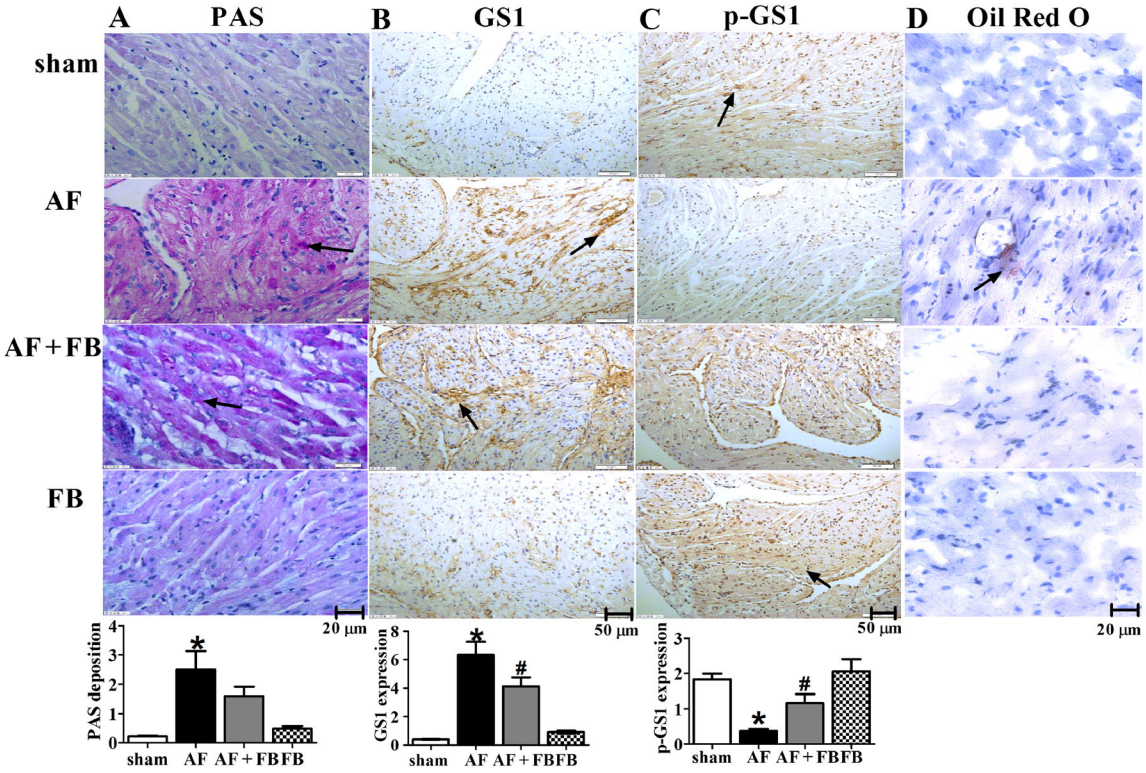

Figure 4

Fenofibrate (FB) reduced the AF-induced accumulation of glycogen and lipid droplets and the expression of glycogen synthase 1 (GS1). (A) Representative images and quantitative analysis of the accumulation of glycogen in all rabbit groups. The magnification is ×40. The glycogen is displayed as red granules in the cardiac tissue. (B) Representative images and quantitative analysis of the expression of the GS1 protein in the atria. (C) Representative images and quantitative analysis of phospho-glycogen synthase1 (p-GS1) protein expression in the atria. The magnification is ×20. (D) Oil Red O was used to visualize lipid droplets in the atrial myocytes. The magnification is ×40. Lipid droplets are stained light red and nuclei are stained blue. *$P < 0.05$ vs. sham group, #$P < 0.05$ versus AF group, $n = 7$ per group.

(100 μM) for 1 h (Huang *et al.*, 2009; Wang *et al.*, 2013) and then stimulated with rapid pacing for 24 h. The PPAR-α, phospho-sirtuin 1 and PGC-1α expression levels were markedly decreased in the rapid pacing HL-1 cells; this effect was inhibited by fenofibrate (Figure 7A, 7B). However, no obvious change in sirtuin 1 expression was observed in the pacing group compared with the control group, whereas fenofibrate up-regulated sirtuin 1 expression (Figure 7A,7B).

Fenofibrate inhibited AF-induced metabolic remodeling through the PPAR-α/sirtuin 1/PGC-1α pathway

To determine whether the inhibitory effect of fenofibrate on atrial metabolic remodeling during AF was dependent on PPAR-α activation, the PPAR-α antagonist GW6471 was used. The HL-1 cells were pretreated with GW6471 (1 μM) for 1 h (Planavila *et al.*, 2011) and then incubated with fenofibrate (100 μM) for 1 h followed by pacing stimulation for 24 h. The expression of PPAR-α, p-sirtuin 1 and PGC-1α was significantly decreased in the GW6471 + FB + pacing group compared with the control group, indicating that GW6471 attenuated the positive effect of fenofibrate on PPAR-α/sirtuin 1/PGC-1α expression in an *vitro* model of AF. The above results demonstrate that fenofibrate inhibits the AF-induced down-regulation of PPAR-α, p-sirtuin 1 and PGC-1α in pacing stimulated HL-1 cells through PPAR-α activation (Figure 7C,7D).

To investigate whether sirtuin 1 was involved in the inhibitory effect of fenofibrate on atrial metabolic remodelling and the relationship between PPAR-α and sirtuin 1, the HL-1 cells were pretreated with the sirtuin 1 specific inhibitor EX527 (10 μM) for 1 h (Zarzuelo *et al.*, 2013) and then treated with fenofibrate (100 μM) for 24 h (Figure 8A, 8B). Fenofibrate abolished the EX527-induced reduction in PPAR-α and p-sirtuin 1 in the HL-1 cells, indicating that PPAR-α positively regulated sirtuin 1 and sirtuin 1 in turn regulated PPAR-α.

The HL-1 cells were pretreated with the sirtuin 1 inhibitor EX527 (10 μM) for 1 h and then treated with fenofibrate (100 μM) for 1 h and stimulated with rapid pacing for 24 h (Figure 8C, 8D). The Western blotting results indicated that AF inhibited the expression of PPAR-α, p-sirtuin 1 and PGC-1α, but fenofibrate reversed this effect. Interestingly, the effect of fenofibrate on the expression of the PPAR-α, p-sirtuin 1 and PGC-1α was attenuated by EX527 (Figure 8C, 8D).

Finally, we assessed the expressions levels of downstream metabolic proteins controlled by the PPAR-α/sirtuin 1/PGC-1α pathway *in vitro*. AF inhibited GLUT4 expression and increased SREBP1 expression; this effect was reversed by fenofibrate (Figure 8C, 8D). However, EX527 attenuated the inhibitory effects of fenofibrate on atrial metabolic remodelling in an *vitro*

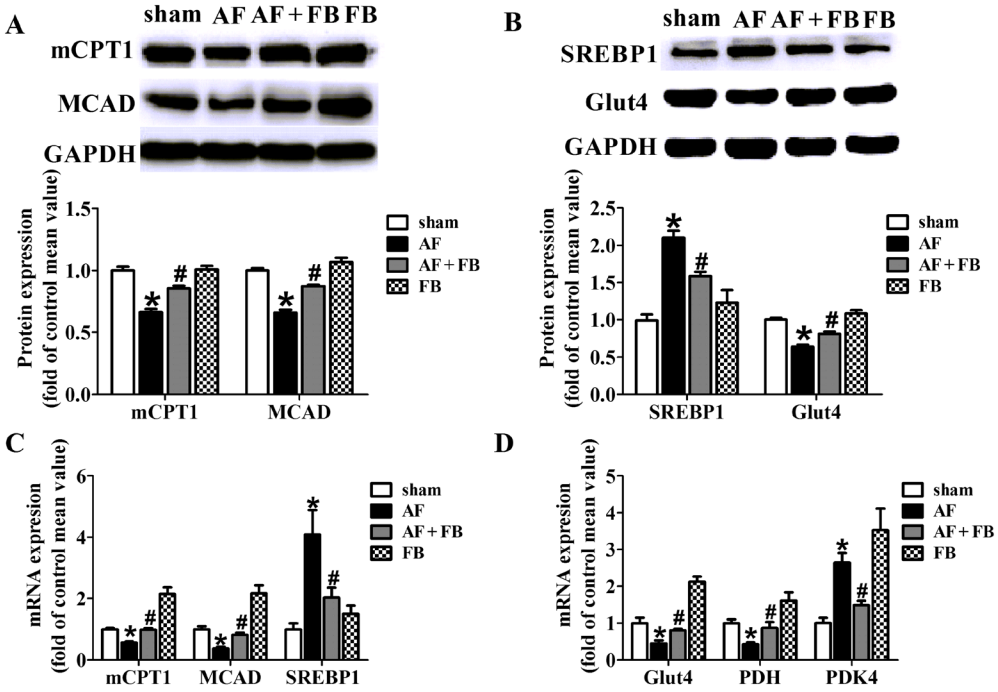

Figure 5

Fenofibrate (FB) inhibited the remodelling of key metabolic factors induced by AF. (A, B) Representative bands and quantification of mCPT1, MCAD, SREBP1 and GLUT4 protein. (C) Quantitative analysis of the expression of the mCPT1, MCAD, SREBP1 genes. (D) Quantitative analysis of the expression of GLUT4, pyruvate dehydrogenase (PDH) and pyruvate dehydrogenase kinase 4 (PDK4) genes. The protein expression was normalized to GAPDH, and the gene expression was normalized to β-actin. *$P < 0.05$ versus sham group, #$P < 0.05$ versus AF group, $n = 7$ per group.

model of AF. The above results indicate that fenofibrate inhibits the atrial metabolic remodelling of AF via a sirtuin 1-dependent pathway. Taken together, our findings suggest that fenofibrate inhibits atrial metabolic remodelling induced by AF by regulating the PPAR-α/sirtuin 1/PGC-1α pathway.

Discussion

The main findings of our present study were that: (1) the PPAR-α, p-sirtuin 1, PGC-1α, mCPT1, MCAD and GLUT4 expression levels were decreased, while the SREBP1 level was increased in AF patients; (2) fenofibrate prevented the down-regulation of mCPT1, MCAD, GLUT4, PDH, PPAR-α, p-sirtuin 1, PGC-1α and the up-regulation of SREBP1 and PDK4 in animal and cell models of AF; and (3) fenofibrate prevented the atrial metabolic remodelling of AF through the PPAR-α/sirtuin 1/PGC-1α pathway.

Previous studies demonstrated abnormal alterations in energy metabolism, such as glycogen accumulation and the reduction of adenine nucleotides, in both animal models and humans with AF (Ausma *et al.*, 2000; Mihm *et al.*, 2001; Tsuboi *et al.*, 2001). Similarly, a significant increase in the atrial blood lactate level was observed during acute AF (van Bragt *et al.*, 2014). Fenofibrate was reported to significantly decrease the level of BOH in high-lipid diet rats (Xu *et al.*, 2014). We demonstrated that AF induced a marked increase in the circulating lactate, AcAc, BOH and TKB levels in rabbits subjected to rapid-pacing for 1 week. The H-FABP, CK and CKMB levels were also significantly increased, indicating that AF-induced ongoing metabolite accumulation and myocardial damage. However, fenofibrate inhibited the metabolite accumulation and myocardial damage during AF, indicating that it has a protective role during AF. Consistent with our findings, the fenofibrate agonist PPAR-α has been shown to have a cardioprotective role against cardiac ischaemia/reperfusion injury (Sugga *et al.*, 2012; Lam *et al.*, 2015). Accordingly, these results indicate that AF-induces metabolic alterations, such as a reduction in adenine nucleotides, the accumulation of glycogen and lipid droplets and an elevation of circulating biochemical metabolites, thereby resulting in ongoing myocardial damage. Fenofibrate inhibited these metabolic alterations via activation of the PPAR-α pathway.

Fenofibrate increases the expression of fatty acid β-oxidation enzymes in the fatty liver (Seo *et al.*, 2008) and reduces SREBP1c expression (Barbieri *et al.*, 2012). Both studies of AF indicated a significant down-regulation of transcripts and proteins involved in lipid metabolism (Barth *et al.*, 2005; Tu *et al.*, 2014). Moreover, recent studies indicated that AF induced an increase in factors involved in lipid droplet formation (Chilukoti *et al.*, 2015). We observed that the levels of mCPT-1 and MCAD were markedly down-regulated in animal model and humans with AF. Conversely, SREBP1 was significantly increased, and there was a rise in the serum H-FABP level followed by a reduction in fatty acid transportation and β-oxidation metabolism. These effects led to reduced ATP and elevated FFA levels and the accumulation of lipid droplets, which were reversed by fenofibrate. The results suggest that AF induced the accumulation of lipid droplets by

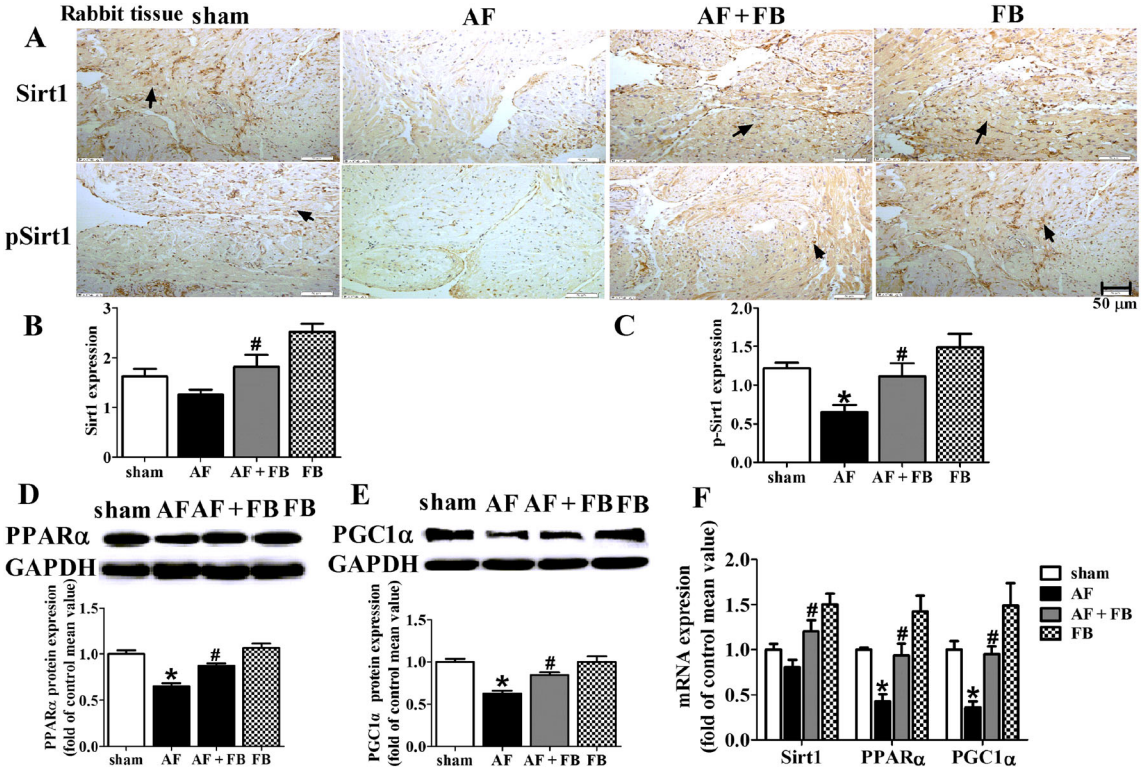

Figure 6

Fenofibrate (FB) prevented the down-regulation of the PPAR-α/sirtuin 1/PGC-1α proteins in AF rabbits. (**A**) Representative images of sirtuin 1 and phospho-sirtuin 1 (p-Sirt1) protein expression in the atria of rabbits. (B, C) Quantitative analysis of the expression of the sirtuin 1 and p-sirtuin 1 protein. (D, E) Representative bands and quantitative analysis of PPAR-α and PGC-1α expression in the atria of rabbits. (F) Quantitative analysis of the expression of the sirtuin 1, PPAR-α, and PGC-1α genes in all groups. The magnification is ×20. *$P < 0.05$ versus sham group, #$P < 0.05$ versus AF group, $n = 7$ per group.

increasing the adipogenesis-related factor SREBP1 and down-regulating fatty acid oxidation. Sirtuin 1 activates PGC-1α to up-regulate fatty acid oxidation genes. PPAR-α and sirtuin 1 were reported to co-regulate the expression of genes promoting fatty acid uptake and oxidation (Planavila *et al.*, 2011). The AF-induced down-regulation of mCPT-1 and MCAD and up-regulation of SREBP1 might have resulted from a reduction in PPAR-α, sirtuin 1 and PGC-1α expression. Consistent with these findings, we found that fenofibrate up-regulated the expression of mCPT1 and MCAD, down-regulated the expression of SREBP1 and reduced the accumulation of lipid droplets in both *in vitro* and *in vivo* models of AF by enhancing the expression of PPAR-α, sirtuin 1 and PGC-1α.

It has been suggested that AF induces a reduction in glucose uptake by decreasing GLUT4 expression, which was associated with β_3 adrenoceptor activation or AMPK and CaMKII activation following glycogen accumulation (Liu *et al.*, 2013; Lenski *et al.*, 2015). In this present study, glycogen accumulation was associated with an abnormal ratio of GS1/p-GS1. Fenofibrate ameliorated this imbalance in GS1/p-GS1 expression, resulting in a reduction in glycogen accumulation. Our findings demonstrated for the first time that PDK4 gene expression was significantly elevated in AF rabbits and that there was an obvious down-regulation of PDH and GLUT4 expression. These effects led to impairments in glucose transportation and TCA cycle metabolism and an increase in the glycolysis pathway, resulting in an elevation of lactate and ketone levels and a reduction of adenine nucleotide levels. Moreover, the inactivation of PDH and ketone bodies to glucose perfusion could induce increasing levels of glycogen synthesis (Kashiwaya *et al.*, 1994; Mayr *et al.*, 2008). Similarly, in our study, AF induced alterations in PDH and PDK4 that contributed to the significant increase in GS1 expression, which was accompanied by a corresponding down-regulation of p-GS1.

Accumulating evidence suggesting that fenofibrate up-regulates the expression of PDK4 and GLUT4 by activating PPAR-α (Okada *et al.*, 2009; Saito *et al.*, 2014) and that resveratrol-activated sirtuin 1 could suppress the activity of PDK4 to enhance PDH activity (Sin *et al.*, 2015). Interestingly, in our study, fenofibrate suppressed the expression of PDK4 and increased the expression of PDH and GLUT4. These effects inhibited the disturbance in GS/p-GS1 expression via PPAR-α activation, resulting in improved glucose metabolism, reduced levels of ketones and lactate, decreased glycogen deposition, the production of more ATP and the consumption of less oxygen.

The PPAR-α agonist fenofibrate prevented the progression of hypertensive heart damage, cardiac hypertrophy, heart failure and lipotoxic cardiomyopathy in addition to its lipid lowering effects; however, the effects of fenofibrate on AF are not known. Our present study found a significant down-regulation of PPAR-α, phospho-sirtuin 1 and PGC-1α

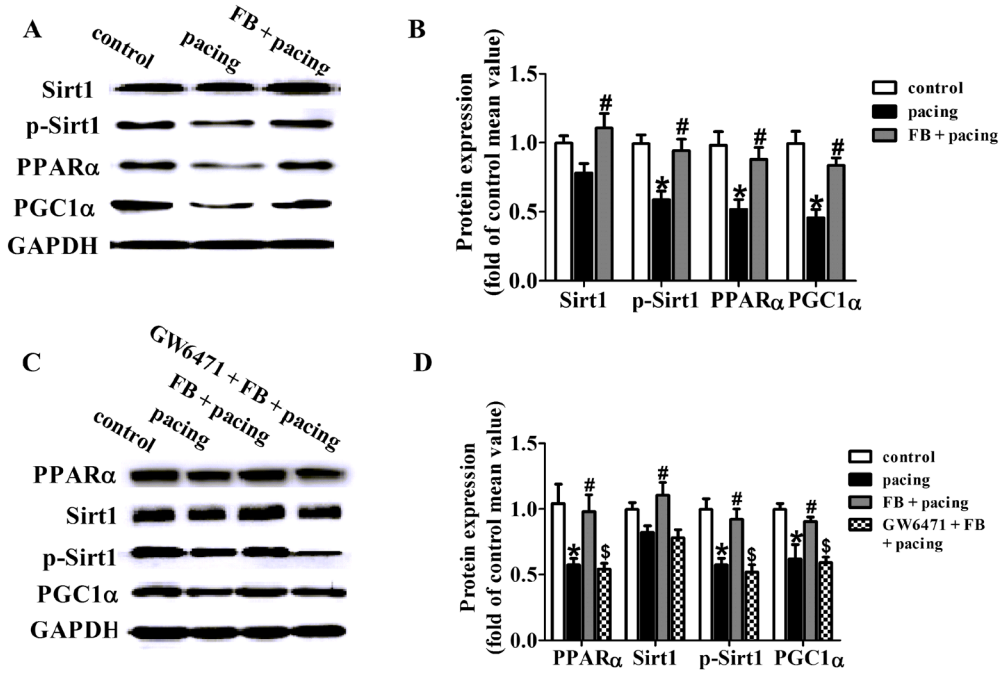

Figure 7

Fenofibrate (FB) improved the metabolic remodelling via a PPAR-α dependent pathway in the AF cellular model. (A) Representative bands of the protein expression of sirtuin 1, p-sirtuin 1, PPAR-α and PGC-1α in HL-1 cells. (B) Quantitative analysis of the expression of sirtuin 1, p-sirtuin 1, PPAR-α and PGC-1α. *$P < 0.05$ versus control group, #$P < 0.05$ versus pacing group. (C) Representative bands of PPAR-α, sirtuin 1, p-sirtuin 1 and PGC-1α expression in pacing cells with or without GW6471 treatment. (D) Quantitative analysis of the expression of PPAR-α, sirtuin 1, p-sirtuin 1 and PGC-1α in all groups. The data were presented as mean ± SEM. *$P < 0.05$ versus control group, $ $P < 0.05$ versus control group, #$P < 0.05$ versus pacing group, (GW6471 + FB + pacing group) $ $P < 0.05$ versus FB + pacing group, #$P < 0.05$ versus GW6471 + FB + pacing group for sirtuin 1 expression. $n = 5$ per group.

expression in cells, rabbits and AF patients. This effect was followed by a reduction in mCPT1, MCAD, GLUT4 and PDH expression and an increase in SREBP1 and PDK4 expression. Interestingly, these small changes in the expression of metabolic factors in AF rabbits induced the derangement of atrial fatty oxidation and glucose metabolism, which was consistent with the findings of our previous study (Meng *et al.*, 2009). Moreover, we demonstrated that fenofibrate up-regulated the expression of PPAR-α, phospho-sirtuin 1 and PGC-1α, resulting in the regulation of down-stream metabolic factors. This effect was abolished by GW6471, indicating that fenofibrate inhibited metabolic factor remodelling through a PPAR-α-dependent pathway. Studies have shown that PPAR-α activated by fenofibrate regulates sirtuin 1 expression (Purushotham *et al.*, 2009; Wang *et al.*, 2013). Moreover, sirtuin 1 and PGC-1α have been proposed as the key regulators of metabolic remodelling in the heart. In this study, fenofibrate prevented the down-regulation of PPAR-α and p-sirtuin 1 induced by EX527, suggesting that PPAR-α positively regulates sirtuin 1.

Resveratrol (an activator of sirtuin 1) has been demonstrated to be cardioprotective agent (Bhullar and Hubbard, 2015; De Angelis *et al.*, 2015). A previous study was reported that resveratrol enhanced sirtuin 1 activity and inhibited the down-regulation of fatty acid oxidation genes via activation of the PPAR-α pathway (Planavila *et al.*, 2011). In the present study, fenofibrate up-regulated p-sirtuin 1 expression via PPAR-α, resulting in the up-regulation of PGC-1α and its key downstream metabolic factors. These effects inhibited the metabolic disturbance in AF and were attenuated by EX527. These findings indicate that fenofibrate mitigated metabolic remodelling during AF by regulating the sirtuin 1 signalling pathway. AMPK and sirtuin 1 are activated by resveratrol and can also be amplified through a reciprocal positive regulatory loop to prevent metabolic stress (Chang and Guarente, 2014). When AMPK is activated, it affects atrial Ca^{2+} handling and contractility and, in particular, protects the atria against metabolic stress (Harada *et al.*, 2015). Fenofibrate has been shown to inhibit inflammation and lipotoxicity by activating PPAR-α and subsequently AMPK (Wang *et al.*, 2013; Hong *et al.*, 2014), indicating that fenofibrate may positively regulate AMPK via activation of PPAR-α and sirtuin 1.

PPAR-α was demonstrated to regulate sirtuin 1 activity in both *vivo* and *vitro* models (Bonzo *et al.*, 2014; Wang *et al.*, 2015). All of the protective effects of sirtuin 1 activation evoked by resveratrol in the heart were lost in PPAR-$\alpha^{-/-}$ mice (Planavila *et al.*, 2011). Moreover, *in vitro* AF model, we observed that blockade of the sirtuin 1 pathway abolished the beneficial effects of fenofibrate. Similarly, blockade of the PPAR-α pathway abolished the effects of the sirtuin 1 pathway on the fatty acid oxidation and glucose metabolism genes. On the basis of our present findings, it is possible that a similar process takes place in the AF setting for the activation of the PPAR-α/sirtuin 1/PGC-1α pathway to promote fatty acid oxidation and glucose metabolism; in turn, PPAR-α and sirtuin 1 reciprocally regulate one another and share many

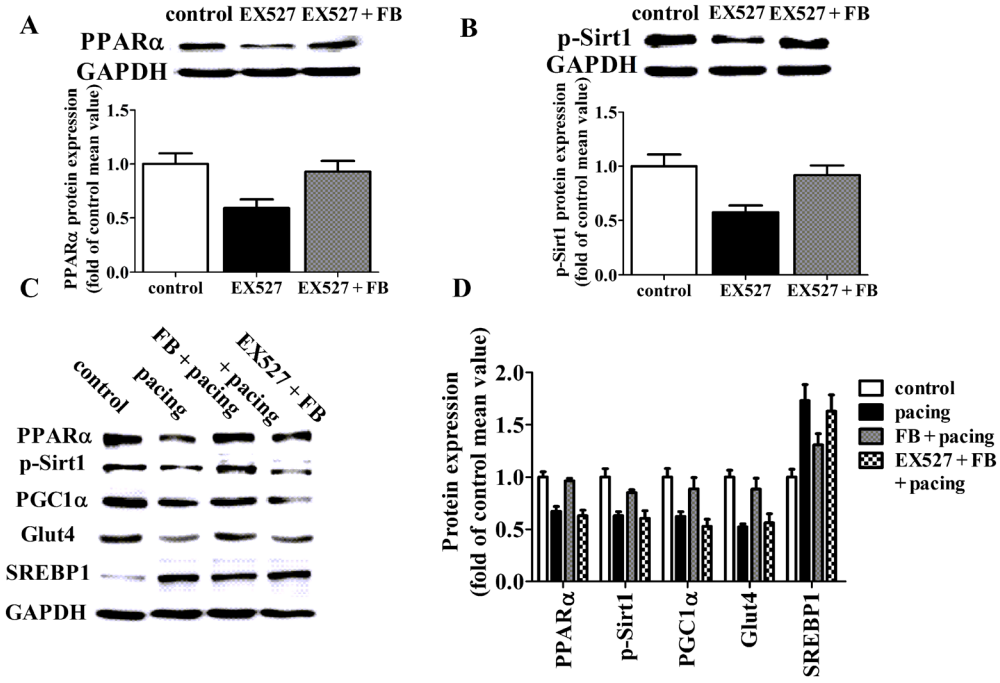

Figure 8

Fenofibrate (FB) inhibited the metabolic remodelling through the PPAR-α/sirtuin 1/PGC-1α pathway in the AF cellular model. (A, B) Representative bands and analysis of PPAR-α and p-sirtuin 1 protein expression in no-pacing HL-1 cells treated with the sirtuin 1 inhibitor EX527 and/or FB. (C) Representative bands of PPAR-α, p-sirtuin 1, PGC-1α, GLUT4 and SREBP1 expression in pacing HL-1 cells pretreated with EX527 and/or FB. (D) Analysis of the expression of, p-sirtuin1, PPAR-α, PGC-1α, GLUT4 and SREBP1 in all groups. $n = 3$ per group.

common target genes, including PGC-1α and key factors involved in fatty acid oxidation and glucose metabolism. Fenofibrate may mimic the effect of resveratrol on modulating the PPAR-α/sirtuin 1/PGC-1α pathway. However, it should be noted that the left atrial size in AF patients was larger than the left atrial size in SR patients, and the impact of atrial dilatation itself on energy metabolism should not be neglected. Therefore, the interpretation of these data should be treated with caution.

Conclusion

We demonstrated that the PPAR-α/sirtuin 1/PGC-1α pathway participates in atrial metabolic remodelling during AF and that fenofibrate inhibits atrial metabolic remodelling by regulating the PPAR-α/sirtuin 1/PGC-1α pathway. Thus, this pathway may provide a novel potential therapeutic target for AF. Our study provides novel insights into the pharmacological role of fenofibrate against AF and atrial metabolic remodelling.

Acknowledgements

This study was supported by the National Natural Science Foundation of China (Nos. 81270252, 81200077 and 81470462), the Foundation for Innovative Research Groups of the National Natural Science Foundation of China (No. 81121003) and the Doctorial Innovation Fund of Harbin Medical University (No. YJSCX2014-30 HYD). We would like to thank Dr. Bai-chun Wang for his cardiac surgery support.

Author contributions

G. Z. L. and T. T. H. designed and conducted the experiments, analysed the data and wrote the manuscript. Y. Y., P. Z. H., J. J. Z., L. S., G. Q. Z., J. M D., X. B. W., H. S., Y. W. L., J. H. Z., Z. X. D., L. Y. and C. C. Z. conducted the experiments. Y. L. and W. M. L designed the experiment and revised the manuscript; and all authors approved the final version of the manuscript.

Conflict of interest

The authors declare no conflicts of interest.

Declaration of transparency and scientific rigour

This Declaration acknowledges that this paper adheres to the principles for transparent reporting and scientific rigour of preclinical research recommended by funding agencies, publishers and other organizations engaged with supporting research.

References

Alexander SPH, Cidlowski JA, Kelly E, Marrion N, Peters JA, Benson HE, *et al.* (2015a). The Concise Guide to PHARMACOLOGY 2015/16: Nuclear hormone receptors. Br J Pharmacol 172: 5956–5978.

Alexander SPH, Fabbro D, Kelly E, Marrion N, Peters JA, Benson HE, *et al.* (2015b). The Concise Guide to PHARMACOLOGY 2015/16: Enzymes. Br J Pharmacol 172: 6024–6109.

Alexander SPH, Kelly E, Marrion N, Peters JA, Benson HE, Faccenda E, *et al.* (2015c). The Concise Guide to PHARMACOLOGY 2015/16: Transporters. Br J Pharmacol 172: 6110–6202.

Asai T, Okumura K, Takahashi R, Matsui H, Numaguchi Y, Murakami H, *et al.* (2006). Combined therapy with PPARalpha agonist and L-carnitine rescues lipotoxic cardiomyopathy due to systemic carnitine deficiency. Cardiovasc Res 70: 566–577.

Ausma J, Coumans WA, Duimel H, Van der Vusse GJ, Allessie MA, Borgers M (2000). Atrial high energy phosphate content and mitochondrial enzyme activity during chronic atrial fibrillation. Cardiovasc Res 47: 788–796.

Barbieri M, Di Filippo C, Esposito A, Marfella R, Rizzo MR, D'Amico M, *et al.* (2012). Effects of PPARs agonists on cardiac metabolism in littermate and cardiomyocyte-specific PPAR-gamma-knockout (CM-PGKO) mice. PLoS One 7: e35999.

Barth AS, Merk S, Arnoldi E, Zwermann L, Kloos P, Gebauer M, *et al.* (2005). Reprogramming of the human atrial transcriptome in permanent atrial fibrillation: expression of a ventricular-like genomic signature. Circ Res 96: 1022–1029.

Bhullar KS, Hubbard BP (2015). Lifespan and healthspan extension by resveratrol. Biochim Biophys Acta 1852: 1209–1218.

Bonzo JA, Brocker C, Jiang C, Wang RH, Deng CX, Gonzalez FJ (2014). Hepatic sirtuin 1 is dispensable for fibrate-induced peroxisome proliferator-activated receptor-alpha function *in vivo*. Am J Physiol Endocrinol Metab 306: E824–E837.

Brundel BJ, Shiroshita-Takeshita A, Qi X, Yeh YH, Chartier D, van Gelder IC, *et al.* (2006). Induction of heat shock response protects the heart against atrial fibrillation. Circ Res 99: 1394–1402.

Casaclang-Verzosa G, Gersh BJ, Tsang TS (2008). Structural and functional remodeling of the left atrium: clinical and therapeutic implications for atrial fibrillation. J Am Coll Cardiol 51: 1–11.

Cha YM, Dzeja PP, Shen WK, Jahangir A, Hart CY, Terzic A, *et al.* (2003). Failing atrial myocardium: energetic deficits accompany structural remodeling and electrical instability. Am J Physiol Heart Circ Physiol 284: H1313–H1320.

Chang HC, Guarente L (2014). SIRT1 and other sirtuins in metabolism. Trends Endocrinol Metabol: TEM 25: 138–145.

Chilukoti RK, Giese A, Malenke W, Homuth G, Bukowska A, Goette A, *et al.* (2015). Atrial fibrillation and rapid acute pacing regulate adipocyte/adipositas-related gene expression in the atria. Int J Cardiol 187: 604–613.

Curtis MJ, Bond RA, Spina D, Ahluwalia A, Alexander SP, Giembycz MA, *et al.* (2015). Experimental design and analysis and their reporting: new guidance for publication in BJP. Br J Pharmacol 172: 3461–3471.

De Angelis A, Piegari E, Cappetta D, Russo R, Esposito G, Ciuffreda LP, *et al.* (2015). SIRT1 activation rescues doxorubicin-induced loss of functional competence of human cardiac progenitor cells. Int J Cardiol 189: 30–44.

Guarente L (2006). Sirtuins as potential targets for metabolic syndrome. Nature 444: 868–874.

Harada M, Tadevosyan A, Qi X, Xiao J, Liu T, Voigt N, *et al.* (2015). Atrial Fibrillation Activates AMP-Dependent Protein Kinase and its Regulation of Cellular Calcium Handling: Potential Role in Metabolic Adaptation and Prevention of Progression. J Am Coll Cardiol 66: 47–58.

Heijman J, Voigt N, Nattel S, Dobrev D (2014). Cellular and molecular electrophysiology of atrial fibrillation initiation, maintenance, and progression. Circ Res 114: 1483–1499.

Hennuyer N, Poulain P, Madsen L, Berge RK, Houdebine LM, Branellec D, *et al.* (1999). Beneficial effects of fibrates on apolipoprotein A-I metabolism occur independently of any peroxisome proliferative response. Circulation 99: 2445–2451.

Hong YA, Lim JH, Kim MY, Kim TW, Kim Y, Yang KS, *et al.* (2014). Fenofibrate improves renal lipotoxicity through activation of AMPK-PGC-1alpha in db/db mice. PLoS One 9: e96147.

Huang XS, Zhao SP, Bai L, Hu M, Zhao W, Zhang Q (2009). Atorvastatin and fenofibrate increase apolipoprotein AV and decrease triglycerides by up-regulating peroxisome proliferator-activated receptor-alpha. Br J Pharmacol 158: 706–712.

Kashiwaya Y, Sato K, Tsuchiya N, Thomas S, Fell DA, Veech RL, *et al.* (1994). Control of glucose utilization in working perfused rat heart. J Biol Chem 269: 25502–25514.

Kilkenny C, Browne W, Cuthill IC, Emerson M, Altman DG (2010). Animal research: reporting *in vivo* experiments: the ARRIVE guidelines. Br J Pharmacol 160: 1577–1579.

Lagouge M, Argmann C, Gerhart-Hines Z, Meziane H, Lerin C, Daussin F, *et al.* (2006). Resveratrol improves mitochondrial function and protects against metabolic disease by activating SIRT1 and PGC-1alpha. Cell 127: 1109–1122.

Lam VH, Zhang L, Huqi A, Fukushima A, Tanner BA, Onay-Besikci A, *et al.* (2015). Activating PPARalpha prevents post-ischemic contractile dysfunction in hypertrophied neonatal hearts. Circ Res 117: 41–51.

Lenski M, Schleider G, Kohlhaas M, Adrian L, Adam O, Tian Q, *et al.* (2015). Arrhythmia causes lipid accumulation and reduced glucose uptake. Basic Res Cardiol 110: 40. doi:10.1007/s00395-015-0497-2.

Li Y, Li WM, Gong YT, Li BX, Liu W, Han W, *et al.* (2007). The effects of cilazapril and valsartan on the mRNA and protein expressions of atrial calpains and atrial structural remodeling in atrial fibrillation dogs. Basic Res Cardiol 102: 245–256.

Li Y, Shi J, Yang BF, Liu L, Han CL, Li WM, *et al.* (2012). Ketamine-induced ventricular structural, sympathetic and electrophysiological remodelling: pathological consequences and protective effects of metoprolol. Br J Pharmacol 165: 1748–1756.

Liang F, Wang F, Zhang S, Gardner DG (2003). Peroxisome proliferator activated receptor (PPAR)alpha agonists inhibit hypertrophy of neonatal rat cardiac myocytes. Endocrinology 144: 4187–4194.

Liu Y, Geng J, Liu Y, Li Y, Shen J, Xiao X, *et al.* (2013). beta3-adrenoceptor mediates metabolic protein remodeling in a rabbit model of tachypacing-induced atrial fibrillation. Cell Physiol Biochem 32: 1631–1642.

Madrazo JA, Kelly DP (2008). The PPAR trio: regulators of myocardial energy metabolism in health and disease. J Mol Cell Cardiol 44: 968–975.

Mayr M, Yusuf S, Weir G, Chung YL, Mayr U, Yin X, *et al.* (2008). Combined metabolomic and proteomic analysis of human atrial fibrillation. J Am Coll Cardiol 51: 585–594.

McGrath JC, Lilley E (2015). Implementing guidelines on reporting research using animals (ARRIVE etc.): new requirements for publication in BJP. Br J Pharmacol 172: 3189–3193.

Meng RS, Pei ZH, Yin R, Zhang CX, Chen BL, Zhang Y, *et al.* (2009). Adenosine monophosphate-activated protein kinase inhibits cardiac hypertrophy through reactivating peroxisome proliferator-activated receptor-alpha signaling pathway. Eur J Pharmacol 620: 63–70.

Mihm MJ, Yu F, Carnes CA, Reiser PJ, McCarthy PM, Van Wagoner DR, *et al.* (2001). Impaired myofibrillar energetics and oxidative injury during human atrial fibrillation. Circulation 104: 174–180.

Okada M, Sano F, Ikeda I, Sugimoto J, Takagi S, Sakai H, *et al.* (2009). Fenofibrate-induced muscular toxicity is associated with a metabolic shift limited to type-1 muscles in rats. Toxicol Pathol 37: 517–520.

Pawson AJ, Sharman JL, Benson HE, Faccenda E, Alexander SP, Buneman OP, *et al.*, NC-IUPHAR(2014). The IUPHAR/BPS guide to PHARMACOLOGY: an expert-driven knowledge base of drug targets and their ligands. Nucleic Acids Res 42: D1098–D1106.

Planavila A, Iglesias R, Giralt M, Villarroya F (2011). Sirt1 acts in association with PPARalpha to protect the heart from hypertrophy, metabolic dysregulation, and inflammation. Cardiovasc Res 90: 276–284.

Purushotham A, Schug TT, Xu Q, Surapureddi S, Guo X, Li X (2009). Hepatocyte-specific deletion of SIRT1 alters fatty acid metabolism and results in hepatic steatosis and inflammation. Cell Metab 9: 327–338.

Saito T, Yamada E, Okada S, Shimoda Y, Tagaya Y, Hashimoto K, *et al.* (2014). Nucleobindin-2 is a positive regulator for insulin-stimulated glucose transporter 4 translocation in fenofibrate treated E11 podocytes. Endocr J 61: 933–939.

Sasaki T, Maier B, Koclega KD, Chruszcz M, Gluba W, Stukenberg PT, *et al.* (2008). Phosphorylation regulates SIRT1 function. PLoS One 3: e4020.

Seiler PU, Stypmann J, Breithardt G, Schulze-Bahr E (2004). Real-time RT-PCR for gene expression profiling in blood of heart failure patients-a pilot study: gene expression in blood of heart failure patients. Basic Res Cardiol 99: 230–238.

Sellevold OF, Jynge P, Aarstad K (1986). High performance liquid chromatography: a rapid isocratic method for determination of creatine compounds and adenine nucleotides in myocardial tissue. J Mol Cell Cardiol 18: 517–527.

Seo YS, Kim JH, Jo NY, Choi KM, Baik SH, Park JJ, *et al.* (2008). PPAR agonists treatment is effective in a nonalcoholic fatty liver disease animal model by modulating fatty-acid metabolic enzymes. J Gastroenterol Hepatol 23: 102–109.

Seppet E, Eimre M, Peet N, Paju K, Orlova E, Ress M, *et al.* (2005). Compartmentation of energy metabolism in atrial myocardium of patients undergoing cardiac surgery. Mol Cell Biochem 270: 49–61.

Sharma NS, Nagrath D, Yarmush ML (2011). Metabolic profiling based quantitative evaluation of hepatocellular metabolism in presence of adipocyte derived extracellular matrix. PLoS One 6: e20137.

Sin TK, Yung BY, Siu PM (2015). Modulation of SIRT1-Foxo1 signaling axis by resveratrol: implications in skeletal muscle aging and insulin resistance. Cell Physiol Biochem 35: 541–552.

Sugga GS, Khan MU, Khanam R (2012). Protective role of fibrates in cardiac ischemia/reperfusion. J Adv Pharm Tech Res 3: 188–192.

Tanno M, Kuno A, Yano T, Miura T, Hisahara S, Ishikawa S, *et al.* (2010). Induction of manganese superoxide dismutase by nuclear translocation and activation of SIRT1 promotes cell survival in chronic heart failure. J Biol Chem 285: 8375–8382.

Tanno M, Sakamoto J, Miura T, Shimamoto K, Horio Y (2007). Nucleocytoplasmic shuttling of the NAD + −dependent histone deacetylase SIRT1. J Biol Chem 282: 6823–6832.

Tsuboi M, Hisatome I, Morisaki T, Tanaka M, Tomikura Y, Takeda S, *et al.* (2001). Mitochondrial DNA deletion associated with the reduction of adenine nucleotides in human atrium and atrial fibrillation. Eur J Clin Invest 31: 489–496.

Tu T, Zhou S, Liu Z, Li X, Liu Q (2014). Quantitative proteomics of changes in energy metabolism-related proteins in atrial tissue from valvular disease patients with permanent atrial fibrillation. Circ J 78: 993–1001.

van Bragt KA, Nasrallah HM, Kuiper M, Luiken JJ, Schotten U, Verheule S (2014). Atrial supply–demand balance in healthy adult pigs: coronary blood flow, oxygen extraction, and lactate production during acute atrial fibrillation. Cardiovasc Res 101: 9–19.

Wang W, Lin Q, Lin R, Zhang J, Ren F, Zhang J, *et al.* (2013). PPARalpha agonist fenofibrate attenuates TNF-alpha-induced CD40 expression in 3T3-L1 adipocytes via the SIRT1-dependent signaling pathway. Exp Cell Res 319: 1523–1533.

Wang WR, Liu EQ, Zhang JY, Li YX, Yang XF, He YH, *et al.* (2015). Activation of PPAR alpha by fenofibrate inhibits apoptosis in vascular adventitial fibroblasts partly through SIRT1-mediated deacetylation of FoxO1. Exp Cell Res 338: 54–63. doi: 10.1016/j.yexcr.2015.07.027.

Xu QY, Liu YH, Zhang Q, Ma B, Yang ZD, Liu L, *et al.* (2014). Metabolomic analysis of simvastatin and fenofibrate intervention in high-lipid diet-induced hyperlipidemia rats. Acta Pharmacol Sin 35: 1265–1273.

Yang Z, Shen W, Rottman JN, Wikswo JP, Murray KT (2005). Rapid stimulation causes electrical remodeling in cultured atrial myocytes. J Mol Cell Cardiol 38: 299–308.

Zarzuelo MJ, Lopez-Sepulveda R, Sanchez M, Romero M, Gomez-Guzman M, Ungvary Z, *et al.* (2013). SIRT1 inhibits NADPH oxidase activation and protects endothelial function in the rat aorta: implications for vascular aging. Biochem Pharmacol 85: 1288–1296.

Zhao J, Li J, Li W, Li Y, Shan H, Gong Y, *et al.* (2010). Effects of spironolactone on atrial structural remodelling in a canine model of atrial fibrillation produced by prolonged atrial pacing. Br J Pharmacol 159: 1584–1594.

Zhao T, Deng YP, Ni M, Chen JK, Li ZP, Li DJ, *et al.* (2014). Fenofibrate improves the impaired endothelial progenitor cell function through inhibiting eNOS uncoupling in diabetic mice. Br J Pharmacol 172: 5704–5728. doi: 10.1111/bph.13054.